

Evaluating Tracking Performance And A New Carrier-to-Noise Estimation Method Using SNACS

Frank M. Schubert, Thomas Jost,
Patrick Robertson
German Aerospace Center (DLR)
Institute of Communications
and Navigation
82234 Wessling, Germany

Roberto Prieto-Cerdeira
European Space Agency, ESA/ESTEC
2201AZ Noordwijk, The Netherlands

Bernard H. Fleury
Aalborg University
Institute of Electronic Systems
DK-9220 Aalborg, Denmark

Abstract—Multipath propagation is still one of the main error sources for many GNSS applications. The introduction of new GNSS signals of Galileo and the modernized GPS, for example, will provide higher signal bandwidths which alleviate the disruptive effects of multipath propagation. To study the influences of highly time-variant channels on GNSS tracking performance, simulations of various environments and signal combinations have to be considered. Many signal studies are based on correlation function simulation techniques. Yet to simulate GNSS signal processing with respect to multipath channels, the time-domain simulation approach serves as the most realistic and accurate but also as the most complex and computationally demanding method. This paper presents the further development of the time-domain GNSS simulation tool SNACS and its extension with additional modulations and GNSS coding schemes. Furthermore, a newly developed loss-of-lock detection method is presented and its performance is evaluated using SNACS.

I. INTRODUCTION

To be able to develop novel techniques for improving the performance of Global Navigation Satellite Systems (GNSS) one has to resort to simulation approaches due to the non-linear nature of the GNSS signal processing chain. Two aspects cause a high computational complexity for GNSS simulations.

Firstly, the GNSS signals' bandwidths are high compared to traditional communication signals. Especially with the advent of new GNSS signals using binary offset carrier (BOC) modulation, a higher processing bandwidth is required. For example, if the Galileo AltBOC(15,10) signal is to be tracked including both main lobes, a two-sided pre-correlation bandwidth of approximately 60 MHz has to be processed. Also, the multiplexed BOC signal class with time-multiplexed (TMBOC) and composite BOC (CBOC) as the representatives for the Global Positioning System (GPS) and Galileo systems, respectively, require higher sampling frequencies than the GPS Coarse Acquisition (C/A) signal needs today.

Secondly, realistic channel models were developed based on wide-band channel sounding measurements. These models mimic the response of the highly time-variant GNSS radio channel in various situations: channel models are for example available for aeronautical [1], land-mobile urban [2][3], suburban [4], for pedestrian [5], and indoor [6] applications. Further, GNSS models based on channel sounding measurements for

multipath scattering caused by vegetation [7] and for indoor location [8] are under development.

The vehicular and pedestrian-type models are able to accurately replay the fierce environments to which a GNSS receiver is exposed in reality. This is the reason why channel models specifically designed for the GNSS use case have received high attention over recent years [9][10]. The consideration of such models is the key to effectively improve GNSS receiver development. However, the computational effort needed to simulate the response of the above channels is very high. An interpolation step has to be introduced to correctly make the transition from the time-continuous channel model domain to the simulation context with its discretized time steps.

In recent years sophisticated software-defined GNSS receivers (SDR) capable of tracking the whole range of present and future GNSS signals have been developed [11][12]. GNSS receivers have to be interfaced to the modern GNSS channel models mentioned above to make a substantiated statement on how different GNSS signals perform in reality.

The Satellite Navigation Radio Channel Signal Simulator (SNACS) was introduced in 2009 as an efficient C++ multiplatform GNSS simulation tool. It performs end-to-end GNSS simulations in time domain consisting of GNSS signal generation, application of time-variant propagation channels, and acquisition and tracking. Such simulations are computationally demanding due to the required high sampling frequencies and the task of above mentioned channel model data transformation [13]. SNACS optimizes the runtime of such simulations by using parallel processing and mathematical libraries. This approach leads to a shorter simulation runtime compared to scripted computer programming languages such as Simulink and MATLAB.

SNACS provides the link between channel models that are realistic but complex to implement and a wide range of software receivers either on signal or correlation function sample level. In addition, tracking loops are included in SNACS, turning it into a convenient tool for the assessment of new GNSS tracking technology.

This paper presents the SNACS evolution from a pure GPS-based tool to a software package able to perform simulations with alternative signals such as CBOC and AltBOC as well.

The paper is organized as follows: Section II describes three common approaches to GNSS signal simulation including time-variant propagation channels. Section III summarizes the key characteristics of the time-domain simulation approach, on which SNACS is based. Section IV introduces a new method for the detection of loss-of-lock events during tracking. This method is compared to a standard method by means of simulation using SNACS.

II. GNSS SIGNAL SIMULATION APPROACHES

Three approaches for GNSS signal simulation that consider realistic time-variant propagation channels can be distinguished: the correlation function peak method, the discriminator function tracking method, and the time-domain simulation method. The former two methods operate on the output of one or more correlators in the GNSS receiver. The third method operates directly on the samples (in the time domain) of the received signal in baseband representation, i.e. the signal that is input to these correlators.

For the following considerations only multipath effects in the channel will be taken into account. Other effects like ionospheric distortions or signal alterations caused by power amplifiers will not be considered. All signals are given in their baseband representation.

The following describes signal processing needed for the usage of time-variant multipath channels in GNSS simulations. The subsequent paragraphs describe the three mentioned simulation methods with respect to the signal processing.

A. Impact of the time-variant multipath channel on GNSS signal transmission

The time-variant response of the channel $h(t, \tau)$ can be written as a sum of multipath components

$$h(t, \tau) = \sum_{i=0}^{N(t)} a_i(t) \cdot \delta(\tau - \tau_i(t)), \quad (1)$$

consisting of $N(t)$ Dirac-impulse-like contributions with time-varying complex weights $a_i(t)$ and delays $\tau_i(t)$.

Denoting the code-division multiple access (CDMA) code signal transmitted by the satellite by $s(t)$ the received signal can be written as

$$r(t) = \int_{-\infty}^{\infty} s(t - \tau) h(t, \tau) d\tau. \quad (2)$$

Inserting (1) into (2) yields

$$r(t) = \sum_{i=0}^{N(t)} a_i(t) s(t - \tau_i(t)). \quad (3)$$

The signal $r(t)$ enters the GNSS receiver's tracking loops.

B. Correlator Output

The receiver always generates $s(t - \tau + \tau_e)$ for the early, $s(t - \tau)$ for the prompt, and $s(t - \tau - \tau_l)$ for the late code shift, respectively. The time span between early and late code replica shifts is denoted as chip spacing $\tau_d = \tau_l - \tau_e$. These

locally replicated signals are then correlated with the incoming signal. With T_c denoting the correlation duration, the output of the correlator at shift τ can be written as

$$C(t, \tau) = \frac{1}{T_c} \int_t^{t+T_c} r(\xi) \cdot s(\xi - \tau) d\xi. \quad (4)$$

Inserting (3) into (4) leads to

$$C(t, \tau) = \frac{1}{T_c} \int_t^{t+T_c} \sum_{i=0}^{N(t)} a_i(\xi) s(\xi - \tau_i(\xi)) s(\xi - \tau) d\xi. \quad (5)$$

Under the assumption that $N(t)$, $a_i(t)$, and $\tau_i(t)$ for $i = 1, \dots, N(t)$, are constant within the integration interval $[t, t + T_c]$,

$$\begin{aligned} N(t') &= N(t) \\ a_i(t') &= a_i(t) \quad , \quad t' \in [t, t + T_c], \\ \tau_i(t') &= \tau_i(t) \end{aligned} \quad (6)$$

(5) can be written as

$$C(t, \tau) = \frac{1}{T_c} \sum_{i=0}^{N(t)} a_i(t) \cdot \int_t^{t+T_c} s(\xi - \tau_i(t)) s(\xi - \tau) d\xi \quad (7)$$

$$= \sum_{i=0}^N a_i(t) \cdot \varphi_{ss}(\tau - \tau_i(t)), \quad (8)$$

when we have defined the autocorrelation function of the transmitted CDMA code signal:

$$\varphi_{ss}(\tau) = \frac{1}{T_c} \int_0^{T_c} s(\xi + \tau) s(\xi) d\xi. \quad (9)$$

We assume that the correlation interval T_c is an integer multiple of the code signal length. For a rectangular pulse shape and unlimited bandwidth, $\varphi_{ss}(\tau)$ is a triangular-shaped function.

For the case of receiving a single signal component (pure line-of-sight, i.e. $N(t) = 0$, $a_0(t) = a_0$, and $\tau_0(t) = \tau_0$) in (3), the output of the correlation operation in the receiver results in $C(t, \tau) = a_0 \varphi_{ss}(\tau - \tau_0)$ according to (8).

However, the multipath channel causes the reception of delayed and weighted versions of $\varphi_{ss}(\tau)$ which distort the cross-correlation $C(t, \tau)$, see (8). The formerly triangular-shaped function appears now as a version with multiple "bulges", depending on the number of propagation paths $N(t)$, the delays $\tau_i(t)$, and the amplitudes $a_i(t)$.

C. Correlation Function Peak Method

The correlation function peak method determines the shift τ for which the correlator output $C(t, \tau)$ reaches its maximum value. This approach assumes that a receiver algorithm estimates the maximum of the correlator output to compute the delay of the incoming signal. The approach can be compared to performing an acquisition for every correlation interval to determine the delay estimation instead of tracking the estimated delay over consecutive correlation intervals. The

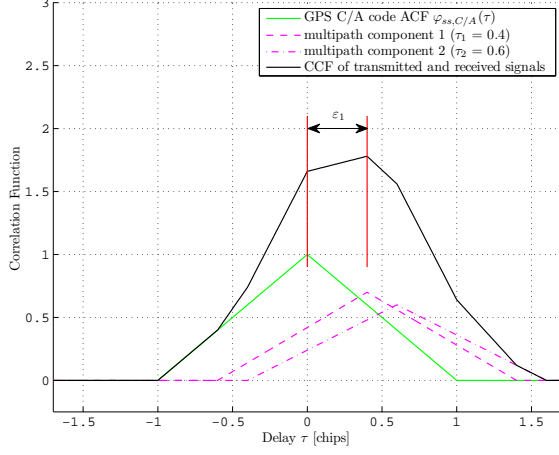


Fig. 1. GPS C/A example for the correlation function peak method. The green and black curves show (8) for the case of one component only and two multipath components, respectively. The resulting deviation from the actual correlation function peak is denoted by ε_1 .

advantage of this approach is that it is independent of the discriminator spacing and other tracking algorithm parameters. Although this method is computationally very efficient it is not realistic due to disregarding an actual correlator spacing and tracking algorithm.

Fig. 1 shows an example of $C(t, \tau)$ for the GPS C/A signal compared with this method. The autocorrelation function of this signal can be approximated by the triangular function

$$\varphi_{ss,C/A}(\tau) = \begin{cases} \tau/T_l + 1 & \text{if } -T_l < \tau \leq 0 \\ -\tau/T_l + 1 & \text{if } 0 < \tau < T_l \\ 0 & \text{otherwise} \end{cases}, \quad (10)$$

where T_l denotes the length of one code chip and when a large processing gain is assumed, i.e. $\varphi_{ss}(t) = 0$ for $\tau \neq [-T_c, T_c]$ [14]. The green curve represents $C(t, \tau) = \varphi_{ss}(\tau)$ for a single-path channel with component characteristics $\tau_0 = 0$, $a_0 = 1$. The black curve represents $C(t, \tau) = 0.7\varphi_{ss}(\tau - 0.4) + 0.6\varphi_{ss}(\tau - 0.6)$ which results in a two-path channel with component characteristics $\tau_0 = 0.4$, $a_0 = 0.7$, $\tau_1 = 0.6$, and $a_1 = 0.6$. In both cases the channel is noise-free.

The cross-correlation function's maximum deviates from the ACF's maximum by ε_1 . This error can be used in the assessment of the impact of distortions caused by multipath components.

D. Discriminator Function Method

The discriminator function method computes prompt, early and late correlation outputs of the incoming signal. From these values, the zero-crossing of the discriminator function can be calculated. The zero-crossing is displaced if multipath is present. This misplacement directly translates into pseudorange estimation errors caused by multipath.

An example of a resulting discriminator function is displayed in Fig. 2. A chip spacing of $\tau_d = 1$ chip is used in this example. The early replica shift is thus given by $\tau_e = -\tau_d/2$

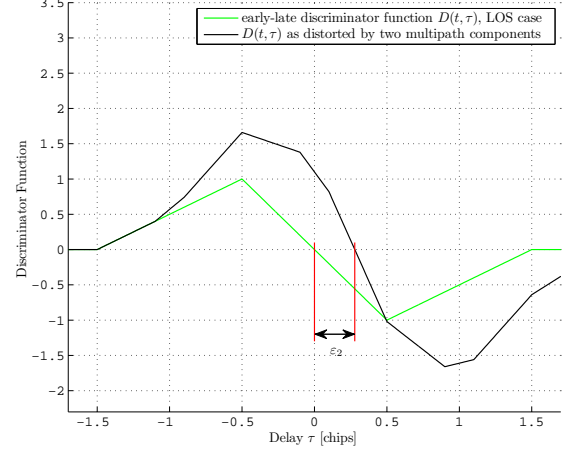


Fig. 2. GPS C/A code example for the discriminator function method. The misplacement ε_2 of the discriminator function's zero crossing is caused by two multipath components.

and the late code replica shift is given by $\tau_l = \tau_d/2$. The early minus late discriminator function for the C/A code is then given by

$$\begin{aligned} D(t, \tau) &= C(t, \tau - \tau_e) - C(t, \tau - \tau_l) \\ &= C\left(t, \tau + \frac{\tau_d}{2}\right) - C\left(t, \tau - \frac{\tau_d}{2}\right). \end{aligned} \quad (11)$$

$D(t, \tau)$ is depicted as green curve in Fig. 2 for the single-path channel as defined in Section II-C. The zero-crossing of this curve is at $\tau = 0$. The black curve reports $D(t, \tau)$ for the two-path channel as defined in Section II-C. The two multipath components introduce a deviation of ε_2 from the zero-crossing at $\tau = 0$. The value of ε_2 is used as an error for the corresponding multipath distortion.

This approach is used for example in [15]. This method is computationally efficient because it can directly compute the cross-correlation values from the signal ACF and the multipath components using (8). An extension of this method uses a delay locked loop (DLL) tracking loop and can thus simulate the behavior of code phase jitter. This results in the development of simulation tools using the so-called fast-simulation method. One example is NavSim [16].

E. Limitations of the Peak and Discriminator Methods

A disadvantage of the two above characterization methods is that both assume that the channel properties such as the multipath component delays and weights stay constant within the correlation interval, see (8). This is due to the fact that $D(t, \tau)$ is determined for every correlation interval in steps of T_c . Changes of the channel that occur within that time period are not taken into account. This assumption is justified in practice for correlation intervals ranging from 1 ms to 4 ms. The maximum possible user speed depends on the frequency of the sampled channel and thus relates directly to the correlation interval time span which can be used.

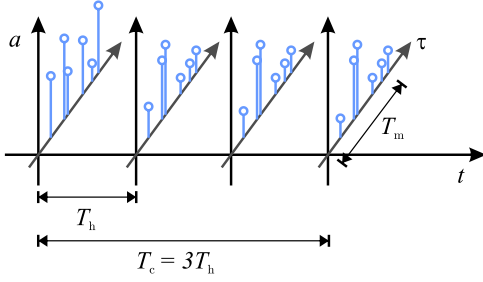


Fig. 3. Example of four channel responses as given out by GNSS channel models. The multipath components are shown as blue Dirac-impulses-like components with complex weight $a(t)$. The channel response update interval is given by T_h and the channel response length is T_m . The correlation interval is denoted by $T_c = n \cdot T_h$ with $n = 3$ in this example.

Neglecting relativistic effects, the Doppler frequency f_D depends on the carrier frequency $f_c = 1.57542$ GHz for the L1 frequency band, the vehicle speed v , and the speed of light c_0 according to $f_D = (v \cdot f_c)/c_0$. According to the Nyquist Theorem, the maximum Doppler frequency present in the channel must satisfy $f_h \geq 2f_D$ where f_h denotes the sampling frequency of the time-variant channel $h(t, \tau)$ with respect to t . Assuming only multipath components caused by non-moving contributors, the maximum vehicle speed is then given by

$$v_m \leq \frac{f_h \cdot c_0}{2 \cdot f_c}. \quad (12)$$

For example, assuming a correlation interval of $T_c = 4$ ms yields a CR update rate of $1/T_c = f_h = 250$ Hz, and with $c_0 \approx 3 \cdot 10^8$ m/s, the maximum possible vehicle speed is $v_{m,4} = 24.80$ m/s ≈ 86 km/h. But for $T_c = 20$ ms, for example, the CR update rate is $1/T_c = f_h = 50$ Hz and the maximum possible vehicle speed is $v_{m,20} = 4.76$ m/s ≈ 17 km/h. This value can be easily exceeded in the land-mobile use case.

Another disadvantage lies in the processing of additive white Gaussian noise (AWGN) and additive interference. Such signals have to be transformed first to be used with correlation function based simulation approaches since AWGN samples are not uncorrelated after the correlation operation anymore.

F. Time-Domain Simulations

A simulation method that takes the signal in the time domain into account can avoid the above mentioned disadvantages of the correlation function based methods. These so-called sample-true or bit-true simulation techniques generate the GNSS signal sample by sample and perform all operations directly on the samples just as in a real receiver. Additionally, AWGN and additive interference can easily be included.

In time-domain the convolution of the generated signal with the channel is independent of the correlation interval. For example, a code with length 4 ms is to be simulated and the correlation interval is chosen to be $T_c = 4$ ms. The channel $h(t, \tau)$ can only be updated at $f_h = 1/(n \cdot T_c) = (250 \text{ Hz})/n$, ($n = 1, 2, 3, \dots$) for the correlation function based simulation methods. For the time domain approach the channel

update rate is not limited to $f_h = 1/(n \cdot T_c)$, higher values such as $f_h = 1$ kHz are possible. Fig. 3 shows an example for $n = 3$ for the above mentioned variables.

A disadvantage is the high computational burden due to the large signal bandwidths. For a GPS C/A code simulation with a single-sided bandwidth of 4 MHz and an intermediate frequency of 10 MHz, a sampling frequency f_s of at least $f_s = 40$ MHz should be used, for example. For a CBOC simulation covering a signal bandwidth of 10 MHz, the simulation sampling frequency should be set to at least 60 MHz. These values were empirically found. For this, simulations using LOS-only scenarios with different sampling frequencies were conducted and the smoothness of the delay estimation was used as evaluation.

A second disadvantage lies in the need for interpolating the time-variant CR, otherwise sub-sample shifts of the multipath-component delays are not possible.

With the discrete-time CR $h_d(t, kT_s)$ where k denotes the absolute sample number in delay and where the sampling interval is denoted by $T_s = 1/f_s$, the interpolation can be written as

$$h_d(t, kT_s) = \sum_{i=0}^N a_i(t) \text{rect}_{[\tau, \tau+T_m]}(kT_s) \text{sinc}[2B(kT_s - \tau_i(t))], \quad (13)$$

with $\text{sinc}(\tau) = \sin(\pi\tau)/(\pi\tau)$ and

$$\text{rect}_{[a,b]}(\tau) = \begin{cases} 1 & \text{if } a \leq \tau \leq b \\ 0 & \text{otherwise} \end{cases}. \quad (14)$$

T_m is the CR length. The usage of the rect function (14) leads to a finite approximation of the sinc function in (13) which is used for the implementation. The resulting $h_d(t, kT_s)$ can then be used as coefficients for a finite impulse response (FIR) filter in the implementation [17]. This convolution with respect to kT_s of the incoming signal and $h_d(t, kT_s)$ is performed in blocks of length $T_h = 1/f_h$:

$$r(t) = \sum_{k=1}^{T_m \cdot f_s} s(t - kT_s) h_d(t, kT_s), \quad (15)$$

for $t = [nT_h, (n+1)T_h], n = 1, 2, 3, \dots$

SNACS was developed to perform accurate and realistic signal simulations for GNSS in the time domain. It was developed in a way to provide simulation results in reasonable time despite the need for high sampling frequencies of time-domain GNSS simulations. Fig. 4 shows the processing modules of the SNACS simulation tool.

III. TIME-DOMAIN SIMULATION OF AN URBAN ENVIRONMENT

SNACS was introduced as an open-source project in [13]. It was extended by separating the GNSS signal generator into a code module and a modulation module. This enables SNACS to generate GPS as well as Galileo signals, in contrast to the GPS-only initial version. SNACS generates the Galileo signals according to [18]. To demonstrate the added signal structures,

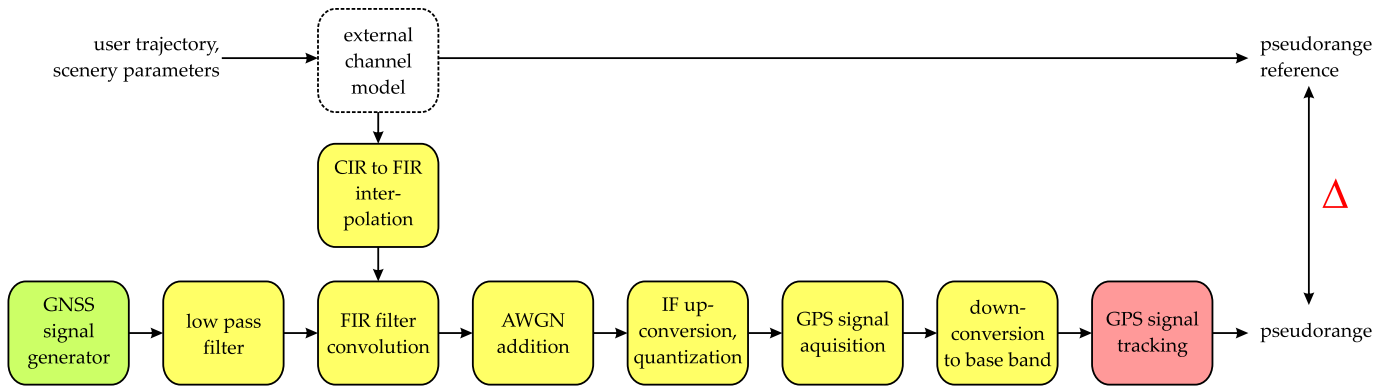


Fig. 4. Overview of the signal processing modules of SNACS.

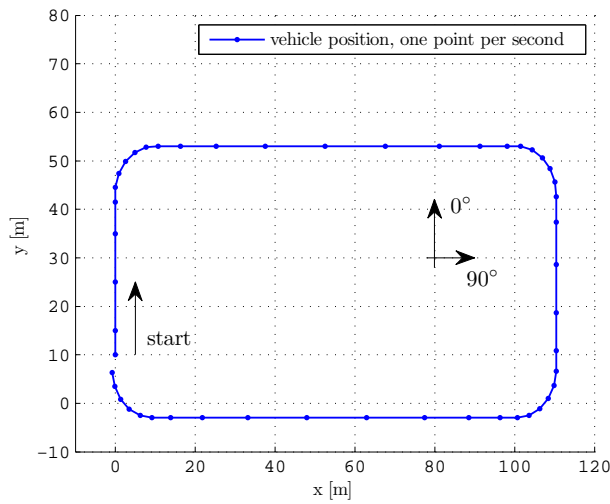


Fig. 5. The defined vehicle trajectory. The vehicle starts at $x = 0$ m, $y = 10$ m. One point per second is plotted on the solid (blue) line representing the trajectory. Thus, the accelerations and decelerations along the trajectory can be seen. The vehicle turns with a constant speed of 3 m/s.

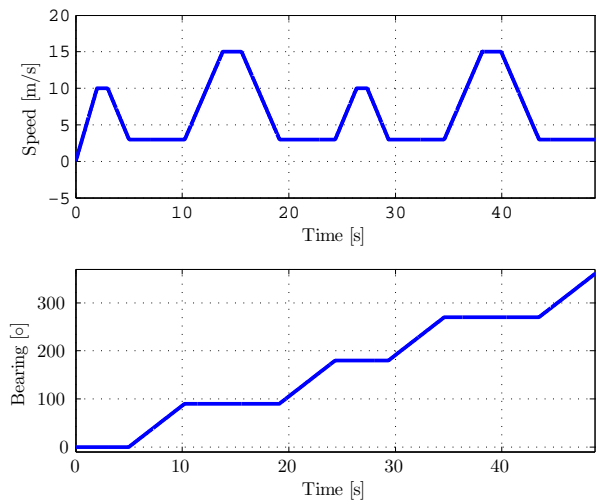


Fig. 6. The vehicle speed and heading are shown in the upper and lower plots, respectively. The heading changes only when the vehicle turns. During the turning times (e.g. $t = 5$ s to $t = 10$ s its speed is constant).

simulations of an urban land-mobile scenario are carried out. The DLR GNSS urban channel model [2] was used for this task.

A vehicle trajectory corresponding to a ride around a street block was defined as depicted in Fig. 5. The vehicle's speed and heading profiles are shown in Fig. 6. The satellite's elevation was set to 30° and its azimuth to 225° with respect to the north direction.

The result of a simulation run is shown in Fig. 7. The drive starts at $t = 0$. The reference in delay is set so that the relative delay of the LOS at $t = 0$ is zero. As the vehicle starts to move away from the starting point, the delay of the line-of-sight (LOS) signal grows larger until the vehicle returns. For the time instants $t = 9 \dots 32$ s shadowing occurs where the signal is attenuated between approximately -20 dB and -40 dB with respect to the unobstructed signal.

Three simulations with the GPS C/A code, the Galileo composite BOC signal CBOC(6,1,1/11), and the E5A BPSK(10)

part of the Galileo AltBOC(15,10) signal were conducted. The simulation parameters are reported in Tab. I. All simulations used 4 Bits as the resolution for the analog-to-digital converter (ADC) and the normalized early-minus-late power as the discriminator function. The tracking algorithm combines a DLL and a phase-locked loop (PLL). The PLL is realized as a Costas loop. The loop bandwidth was set to 5 Hz for the DLL and 25 Hz for the PLL. The simulations were performed without noise in order to assess the influence of the time-variant multipath channel only.

The results are shown in Fig. 8, Fig. 9, and Fig. 10 for the C/A, the CBOC, and the AltBOC simulations, respectively. The C/A tracking result shows a high code phase jitter due to its large early-late spacing of 1 chip. These three simulations serve not as a direct comparison of the tracking performance of the above mentioned signals but rather outline the extended signal capabilities of SNACS. Although the time span from $t \approx 9$ s to $t \approx 31$ s where the LOS signal is highly attenuated,

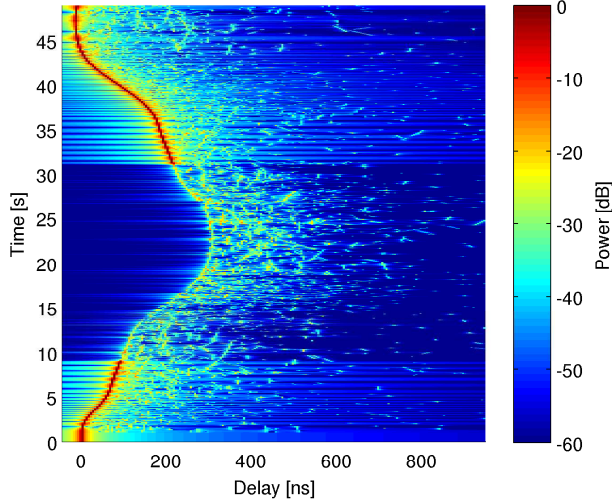


Fig. 7. Realization of the DLR land-mobile urban channel model which was used for the simulations. The line-of-sight signal is shown as the strongest path in red color. From $t = 9$ s until $t = 32$ s it was shadowed by buildings.

TABLE I
SIMULATION PARAMETERS

	GPS C/A	CBOC	AltBOC
Sampling frequency	40 MHz	60 MHz	80 MHz
Intermediate frequency	10 MHz	15 MHz	20 MHz
Pre-correlation bandwidth	8 MHz	10 MHz	10 MHz
Correlation interval	1 ms	4 ms	1 ms
Early-late spacing	1 chips	0.4 chips	0.5 chips

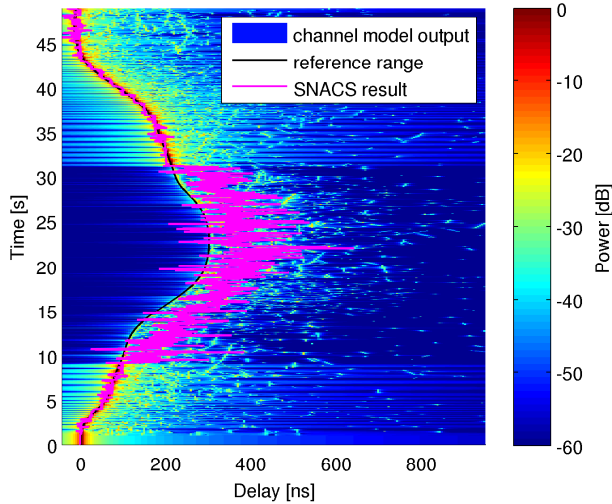


Fig. 8. Pseudorange result of a GPS C/A signal simulation using the DLR land-mobile urban channel model.

all simulations stay in the locked state. The delay estimation result is seen to be jumping due to the signal reflections leading to errors of up to 90 ns. The DLL stays in lock by using the energy that the multipath components contribute to the

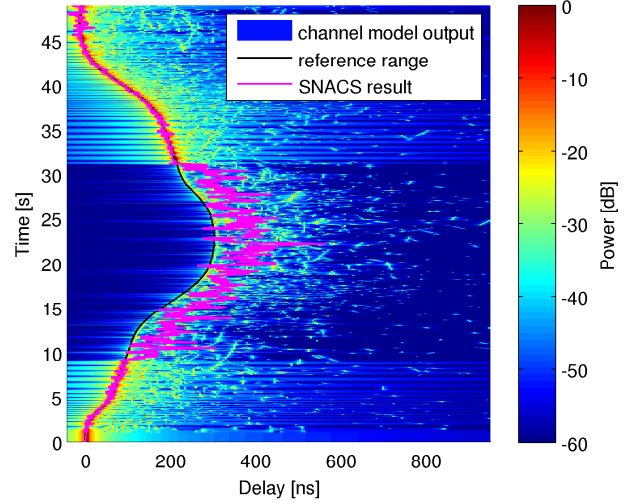


Fig. 9. Pseudorange result of a Galileo CBOC signal simulation using the DLR land-mobile urban channel model.

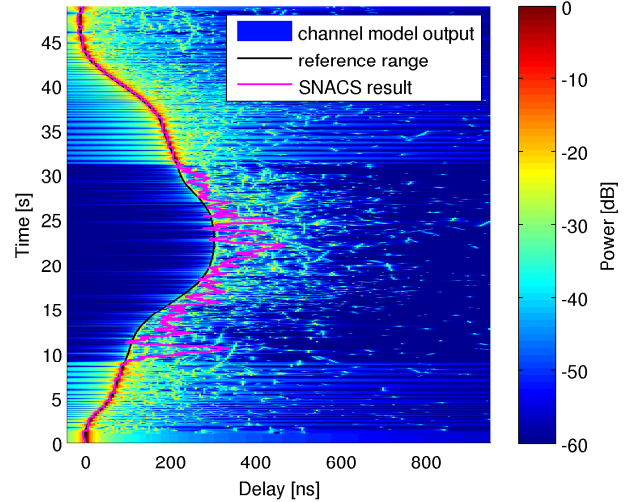


Fig. 10. Pseudorange result of a Galileo AltBOC signal simulation using the DLR land-mobile urban channel model.

received signal.

IV. A NEW C/N_0 ESTIMATION METHOD

A. Standard Method

The standard method to detect whether a DLL tracks a satellite's signal determines the signal-to-noise ratio (SNR) within two different bandwidths [19]. These two values can be used to estimate the current C/N_0 which in turn can be used to detect if a DLL is tracking a signal or if it has lost its lock to the maximum of the correlation peak. For example, if the C/N_0 value drops below a certain threshold, for instance 10 dB-Hz, a loss-of-lock event could be declared and the GNSS receiver would initiate a re-acquisition of the satellite signal. Loss-of-lock detection is thus related to C/N_0 estimation.

The standard method as outlined in [19] is repeated for clarity. First, the SNR value is calculated by using a broader bandwidth as

$$\text{SNR}_{W,k} = \left(\sum_{i=1}^M (I_i^2 + Q_i^2) \right)_k, \quad (16)$$

then the SNR for a narrow bandwidth

$$\text{SNR}_{N,k} = \left(\sum_{i=1}^M I_i \right)_k^2 + \left(\sum_{i=1}^M Q_i \right)_k^2, \quad (17)$$

where I_i and Q_i are the inphase and quadrature components of the prompt correlation result, is obtained. The results are averaged over M correlation periods. Then for every k , the quotient

$$P_k = \frac{\text{SNR}_{N,k}}{\text{SNR}_{W,k}} \quad (18)$$

is determined. In the next step, the sample average of K of such P_k values is computed, yielding

$$\mu_P = \frac{1}{K} \sum_{k=1}^K P_k. \quad (19)$$

The final C/N_0 value can be computed to

$$C/N_0 = 10 \log_{10} \left(\frac{1}{T_c} \frac{\mu_P - 1}{M - \mu_P} \right), \quad (20)$$

where T_c denotes the correlation interval, for example $T_c = 1$ ms in the case of a GPS receiver tracking the C/A code as shown in Tab. I.

B. New Method

The new proposed method redefines (16) to

$$\text{SNR}_{W,k} = \left[\sum_{i=1}^M \left(|I_i + jQ_i| - \sqrt{\frac{\pi}{2}} \right)^2 \right]_k \quad (21)$$

and (17) becomes

$$\text{SNR}_{N,k} = \left[\sum_{i=1}^M \left(|I_i + jQ_i| - \sqrt{\frac{\pi}{2}} \right)^2 \right]_k. \quad (22)$$

The equations (20) and (19) for the C/N_0 calculation stay unchanged.

The advantage of using (21) and (22) is that they are not affected by the phase $\alpha_{Z,i}$ of the complex number $Z_i = I_i + jQ_i$, the complex prompt correlator output at temporal increasing index i . Due to physical movement of the receiver, uncompensated Doppler results in a steadily increasing or decreasing of $\alpha_{Z,i}$ over time index i . Hence, the summation over I_i and Q_i performed in (17) tends to zero. In this case $\text{SNR}_{N,k}$ is small and decreases the estimated C/N_0 in (20) and results in a false alarm for the lock detector.

The new method takes the absolute value of Z_i and omits the phase rotation introduced by the receiver movement. Generally, taking the absolute value has the disadvantage that the average over Z_i in the white noise only case will not

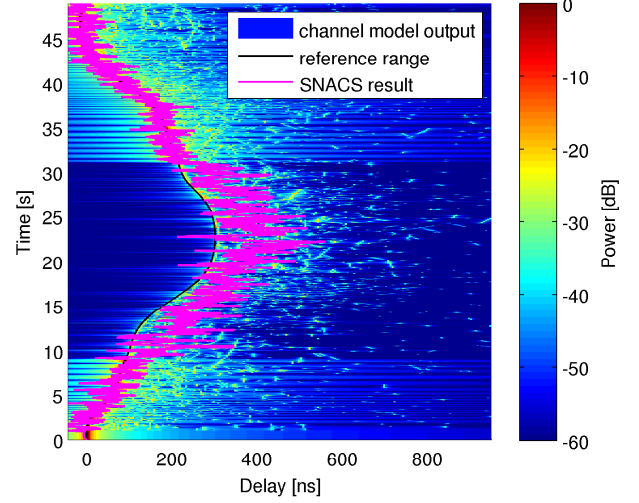


Fig. 11. Channel response as given in Fig. 7 and delay estimation as simulated by SNACS. The noise generator was set to 35 dB-Hz. The noise generator was disabled for simulation times $t < 1$ s and activated after that time.

be zero any more. Therefore taking only the absolute value of Z_i would produce missed alarms. According to [19] the distribution of the noise part of Z_i is complex Gaussian with known variance. Hence taking the absolute value of the noise part in Z_i results in a Rayleigh distributed random variable with a mean value of $\sqrt{\pi/2}$. In order to minimise the number of missed alarms, this mean value is subtracted in (21) and (22).

C. Simulation Results

Two simulation runs using the GPS C/A signal were carried out to compare the performance of the standard method and the proposed method. Both example use $M = 10$ and $K = 50$ for the equations in the following considerations. The C/N_0 was set to 35 dB-Hz in both cases. The noise generator was disabled in the time interval $[0, 1]$ s. The remaining parameters are given as $T_c = 0.001$ s, an early-minus-late-normalized DLL discriminator and an early-late spacing of 1 chip.

The channel response as depicted in Fig. 7 was used for the first simulation. Fig. 11 shows the estimated delay versus time as simulated by SNACS. Fig. 12 shows a comparison between the standard and the proposed C/N_0 estimation method in the upper plot. The lower plot shows the pseudorange speed between vehicle and transmitter versus time. This speed is not the absolute speed of the vehicle as reported in the upper plot of Fig. 6 but the relative speed between vehicle and transmitter and is hence different.

It can be seen that during situations with low C/N_0 and at times when the receiver is moving that the standard method outputs C/N_0 values below 0 dB-Hz at $t = 2$ s...6 s. If a loss-of-lock detector would have a threshold at 15 dB-Hz, it would have declared out of lock multiple times during this situation. The proposed method on the other hand is less susceptible to the receiver movement and these low- C/N_0 situation. It

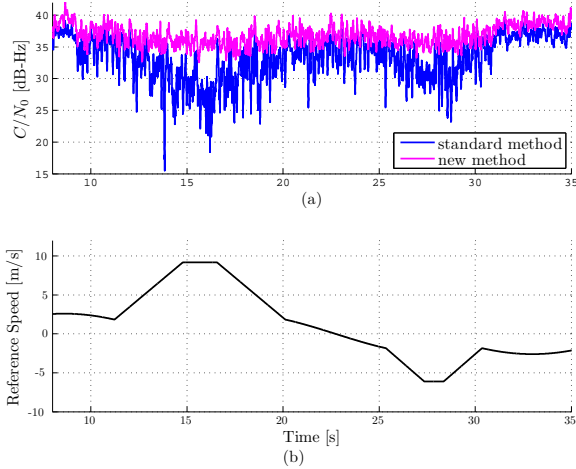


Fig. 12. The upper plot (a) depicts the C/N_0 estimation versus time with the standard (blue) and the new (magenta) method for the realization of the DLR urban channel model as shown in Fig. 7. The reference range speed is shown in plot (b).

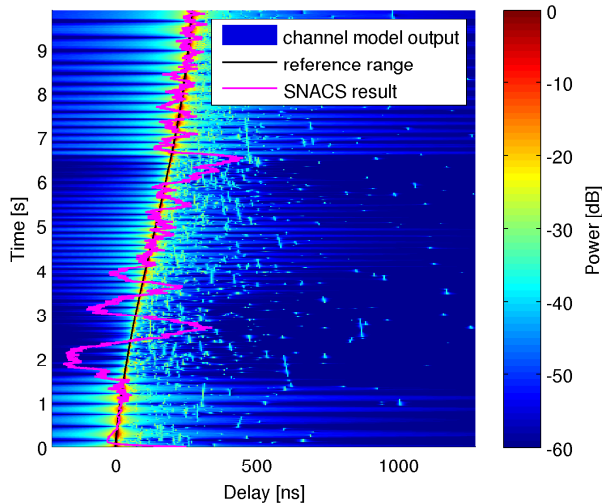


Fig. 13. CR generated with the DLR urban land-mobile in a second scenario channel and delay estimates computed with SNACS.

computes a higher value that stays in between 33 dB-Hz and 39 dB-Hz. A threshold of 15 dB-Hz is not undercut.

The second simulation run uses another realization of the DLR urban channel model with slowly accelerating and decelerating vehicle trajectory. The channel response is shown in Fig. 13 together with the estimated delay versus time as simulated by SNACS. The comparison of standard and new C/N_0 estimation method is reported in Fig. 14 in the upper plot. The lower plot shows the reference speed between vehicle and transmitter versus time.

V. IMPLEMENTATION

SNACS is implemented in the C++ programming language. It uses a thoroughly designed object-oriented approach. Every

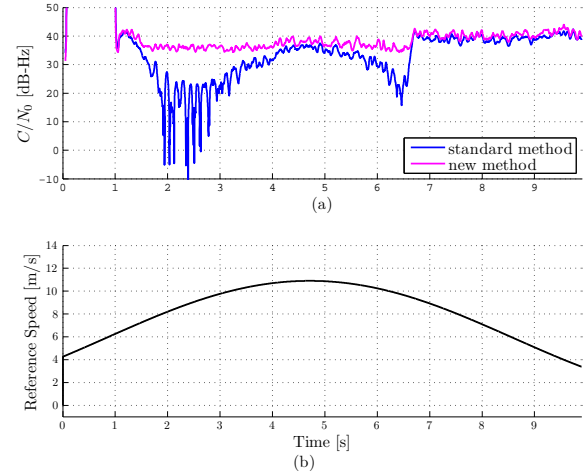


Fig. 14. Plot (a) depicts the C/N_0 estimate versus time with the standard (blue) and the new (magenta) method for the second propagation scenario. The reference range speed is shown in plot (b).

signal processing module operates in its own thread. The samples are passed in buffers from module to module for asynchronous access. This limits the need for time and memory consuming storage of the signal.

Additionally, multi-threading is used for critical computations such as for the calculation of the correlation in the tracking module and for the convolution process in the channel module.

In contrast to the initial GPS-only version [13], SNACS can now process a range of GNSS signals. It uses one class hierarchy with abstract base-classes for signal modulations and one for GNSS codes, respectively. All types of modulation, such as BPSK, BOC, CBOC, and AltBOC are computed using the absolute time as input parameter. The same applies to the code generation modules, which generate the code variants C/A, E1B, E1C, and the E5 codes. This way, all combinations of implemented modulation and code variants can be simulated with SNACS.

Moreover, different types of signals can be used in the signal generation module and the tracking module. For example, the tracking of a CBOC(6, 1, 1/11) signal using a BOC(1,1) signal can easily be implemented.

Also, additional modules are available. For example a multiplicative module for the simulation of ionospheric scintillations, as demonstrated in [20], or a module for the application of channel sounding measurements.

SNACS runs on the operating system Linux and Windows. A screenshot of the channel interpolation module, the incoming signal processing module, and the correlation result of a simulation is shown in Fig. 15. SNACS has been published as an open-source software. The new updates are available on the project website [21].

VI. CONCLUSION

The effects of time-variant multipath channels on GNSS receiver tracking were described. A comparison of correlation

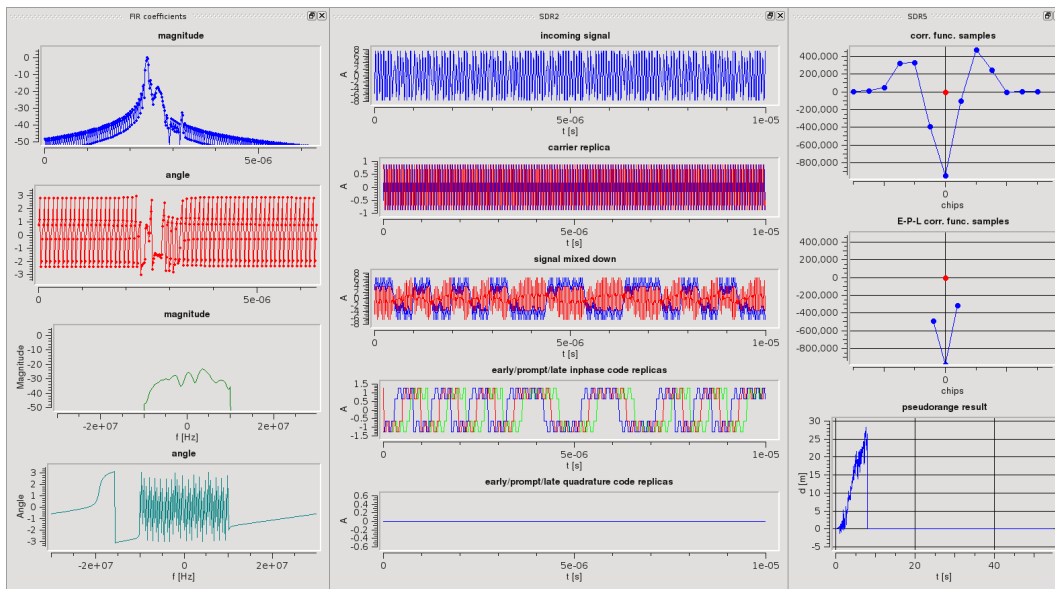


Fig. 15. Screenshot of a running SNACS simulation using the CBOC signal and the DLR land-mobile urban channel model. Only the visualization of three processing modules are shown: The output of the CR interpolation as FIR coefficients is shown on the left, the code replica generation is shown in the center, and the correlation function samples and pseudorange result are displayed on the right.

function-based GNSS simulation approaches with the time-domain method was given. The concept behind time-domain simulation was described. The extension of BOC modulation and Galileo ranging codes for the SNACS GNSS signal simulation software was introduced. Simulations using GPS, CBOC, and AltBOC and a highly fluctuating channel in an urban setting demonstrated the tracking behavior of these signals.

The problem of reliable C/N_0 estimation and thus the knowledge of whether a tracking loop is in lock or not in situations with signal Doppler shifts was addressed by the introduction of a new C/N_0 estimation method. As an exemplary SNACS simulation showed this method performs better than the standard method for moving receivers in multipath environments.

The presented enhancements for SNACS allow for the highly realistic simulation of many BOC modulated signals as transmitted by the new and modernized GNSS constellations. For the future, the joint tracking of inphase and quadrature GNSS codes and pilot signals promise a gain while tracking signals which are distorted by multipath reception. Other additions to SNACS will comprise multi-link simulations and innovative tracking techniques such as tracking using a particle filter.

REFERENCES

- [1] A. Steingass, A. Lehner, F. Pérez-Fontán, E. Kubista, and B. Arbesser-Rastburg, "Characterization of the aeronautical satellite navigation channel through high-resolution measurement and physical optics simulation," *International Journal of Satellite Communications and Networking*, vol. 26, 2008.
- [2] A. Lehner, "Multipath channel modelling for satellite navigation systems," Ph.D. dissertation, Universität Erlangen-Nürnberg, 2007.
- [3] F. Pérez-Fontán, M. Vázquez-Castro, C. Cabado, J. García, and E. Kubista, "Statistical modeling of the LMS channel," *IEEE Transactions on Vehicular Technology*, vol. 50, no. 6, pp. 1549–1567, 2001.
- [4] A. Steingass and A. Lehner, "Navigation in multipath environments for suburban applications," in *Proceedings of the 20th International Technical Meeting of the Institute of Navigation Satellite Division*, Fort Worth, Texas, USA, 2007.
- [5] A. Lehner, A. Steingass, and F. Schubert, "A location and movement dependent GNSS multipath error model for pedestrian applications," in *Proceedings of the 13th European Navigation Conference*, Naples, Italy, 2009.
- [6] M. Paonni, V. Kropp, A. Teuber, and G. Hein, "A new statistical model of the indoor propagation channel for satellite navigation," in *Proceedings of the International Technical Meeting of the Institute of Navigation (ION GNSS 2008)*, Savannah, Georgia, USA, 2008.
- [7] F. Schubert, B. H. Fleury, P. Robertson, R. Prieto-Cerdeira, A. Steingass, and A. Lehner, "Modeling of multipath propagation components caused by trees and forests," in *Proceedings of the 4th European Conference on Antennas and Propagation*, Barcelona, Spain, 2010.
- [8] T. Jost and W. Wang, "Satellite-to-indoor broadband channel measurements at 1.51 GHz," in *Proceedings of the 2009 International Technical Meeting (ITM) of the Institute of Navigation*, Anaheim, California, USA, 2009.
- [9] B. Krach and G. Artaud, "Performance assessment of navigation signals in realistic multipath environments," in *Proceedings of Navitec 2008*, Noordwijk, Netherlands, 2008.
- [10] M. Vergara, F. Antreich, G. Artaud, M. Meurer, and J.-L. Issler, "On performance assessment of GNSS receivers," in *Proceedings of the International Technical Meeting of the Institute of Navigation (ION GNSS 2009)*, Savannah, Georgia, USA, 2009.
- [11] K. Borre, D. Akos, N. Bertelsen, P. Rinder, and S. Jensen, *A Software-Defined GPS and Galileo Receiver – A Single-Frequency Approach*. Birkhäuser Boston, 2007.
- [12] G. Artaud, G. Menard, L. Ries, J. Dantepal, and J.-L. Issler, "Juzzle software receiver," in *Proceedings of Navitec 2006*, Noordwijk, The Netherlands, 2006.
- [13] F. Schubert, R. Prieto-Cerdeira, P. Robertson, and B. Fleury, "SNACS - the satellite navigation radio channel signal simulator," in *Proceedings of the International Technical Meeting of the Institute of Navigation (ION GNSS 2009)*, Savannah, Georgia, USA, 2009.
- [14] P. Misra and P. Enge, *Global Positioning System: Signals, Measurements, and Performance*, 2nd ed. Ganga-Jamuna Press, 2006.
- [15] M. Irsigler, J. A. Avila-Rodriguez, and G. W. Hein, "Criteria for

- GNSS multipath performance assessment,” in *Proceedings of the 18th International Technical Meeting of the Institute of Navigation (ION GNSS)*, Long Beach, CA, USA, 2005.
- [16] J. Furthner, E. Engler, A. Steingass, M. Angermann, J. Hahn, A. Hornbostel, R. Krämer, H. P. Müller, T. Noack, P. Robertson, S. Schlüter, and J. Selva, “Realization of an end-to-end software simulator for navigation systems,” *International Journal of Satellite Communications, Special Issue: Satellite Navigation and Positioning*, 2000.
- [17] W. H. Tranter, K. S. Shanmugan, T. S. Rappaport, and K. L. Kosbar, *Principles of Communication Systems Simulation*. Prentice Hall, 2004.
- [18] *Galileo Open Service Signal In Space Interface Control Document*, European Space Agency / European GNSS Supervisory Authority Std. OS SIS ICD Draft 1, 2008.
- [19] B. W. Parkinson and J. J. Spilker, *Global Positioning System: Theory and Applications*. American Institute of Aeronautics and Astronautics, 1996.
- [20] R. Prieto-Cerdeira, F. M. Schubert, F. Amarillo, and M. Crisci, “Ionospheric scintillations: Simulation, performance verification and analysis of detection algorithms on GNSS receivers,” in *Proceedings of the 2nd International Colloquium - Scientific and Fundamental Aspects of the Galileo Programme*, Padua, Italy, 2009.
- [21] F. M. Schubert, *SNACS – The Satellite Navigation Radio Channel Signal Simulator*, 2009, <http://snacs.sourceforge.net>.